inorganics

MDPI

Article

Kinetic Studies of Sodium and Metforminium Decavanadates Decomposition and In Vitro Cytotoxicity and Insulin- Like Activity

Aniela M. Silva-Nolasco [1,2], Luz Camacho [2], Rafael Omar Saavedra-Díaz [1], Oswaldo Hernández-Abreu [1], Ignacio E. León [3] and Irma Sánchez-Lombardo [1,*]

1 Centro de Investigación de Ciencia y Tecnología Aplicada de Tabasco, División Académica de Ciencias Básicas (CICTAT), Universidad Juárez Autónoma de Tabasco, Carretera Cunduacán-Jalpa km. 1 Col. La Esmeralda, Cunduacán 86690, Tabasco, Mexico; animonsino@gmail.com (A.M.S.-N.); rafael.saavedra@ujat.mx (R.O.S.-D.); oswaldo.hernandez@ujat.mx (O.H.-A.)

2 Laboratorio de Nutrición Experimental, Instituto Nacional de Pediatría, Ciudad de Mexico 04530, Mexico; camacho.luz@gmail.com

3 Centro de Química Inorgánica CEQUINOR (CONICET, UNLP), Bv 120 1465, La Plata 1900, Argentina; iel86@yahoo.com.ar

* Correspondence: irma.sanchez@ujat.mx

Received: 22 October 2020; Accepted: 2 December 2020; Published: 8 December 2020

Abstract: The kinetics of the decomposition of 0.5 and 1.0 mM sodium decavanadate (NaDeca) and metforminium decavanadate (MetfDeca) solutions were studied by ^{51}V NMR in Dulbecco's modified Eagle's medium (DMEM) medium (pH 7.4) at 25 °C. The results showed that decomposition products are orthovanadate $[H_2VO_4]^-$ (V_1) and metavanadate species like $[H_2V_2O_7]^{2-}$ (V_2), $[V_4O_{12}]^{4-}$ (V_4) and $[V_5O_{15}]^{5-}$ (V_5) for both compounds. The calculated half-life times of the decomposition reaction were 9 and 11 h for NaDeca and MetfDeca, respectively, at 1 mM concentration. The hydrolysis products that presented the highest rate constants were V_1 and V_4 for both compounds. Cytotoxic activity studies using non-tumorigenic HEK293 cell line and human liver cancer HEPG2 cells showed that decavanadates compounds exhibit selectivity action toward HEPG2 cells after 24 h. The effect of vanadium compounds (8–30 μM concentration) on the protein expression of AKT and AMPK were investigated in HEPG2 cell lines, showing that NaDeca and MetfDeca compounds exhibit a dose-dependence increase in phosphorylated AKT. Additionally, NaDeca at 30 μM concentration stimulated the glucose cell uptake moderately (62%) in 3T3-L1 adipocytes. Finally, an insulin release assay in βTC-6 cells (30 μM concentration) showed that sodium orthovanadate (MetV) and MetfDeca enhanced insulin release by 0.7 and 1-fold, respectively.

Keywords: polyoxometalates; decavanadate; cytotoxicity; insulin-like activity; diabetes therapy; vanadium biochemistry; vanadium speciation

1. Introduction

Polyoxometalates (POMs) have several applications in biology and medicine. Interactions between the highly charged POM molecules and biological molecules frequently occur through hydrogen-bonding and electrostatic interactions [1]. Moreover, POMs have shown pharmacological activities in vitro and in vivo, such as antitumor, antimicrobial, and antidiabetic [2,3]. Their roles in biological systems are non-functional or functional kind of interactions with biomolecules [4], like the tungstate cluster that helps to solve the X-ray structure of ribosome [5] or the insulin-like properties of the decavanadates [6].

In recent years, several organic and inorganic decavanadate compounds have been synthesized, exhibiting a wide structural supramolecular diversity in one, two or three dimensions [7–9]. However, the interaction of decavanadates with biological targets under physiological conditions are scarce reported since the decavanadate anion can be formed at vanadium concentrations up to 0.1 mM and in the pH range of 2–6 [10], and some organic decavanadates compounds are water-insoluble [11].

In biological studies, buffer solutions are extensively used, although just a few studies have addressed the speciation of the decomposition products of the decavanadate compounds in such reaction media. The decomposition of the decameric species at neutral pH can be followed by ^{51}V NMR showing a decrease in the peaks associated with the three magnetic independent vanadium nuclei of the decavanadate V_A, V_B and V_C (Figure 1), albeit an increase of the signals for the metavanadate peak $[H_2VO_4]^-$ (V_1) and the appearance of the orthovanadates species signals like $[H_2V_2O_7]^{2-}$ (V_2), $[V_4O_{12}]^{4-}$ (V_4) and $[V_5O_{15}]^{5-}$ (V_5) [12–14]. Moreover, monomeric vanadate is always present in decavanadate solutions at neutral pH [15]. The decavanadate decomposition rate is faster in acid than in basic solutions [16,17]. In the latter, the reaction proceeds via base-dependent or base-independent paths, and it depends on the counterions present in the solution [17].

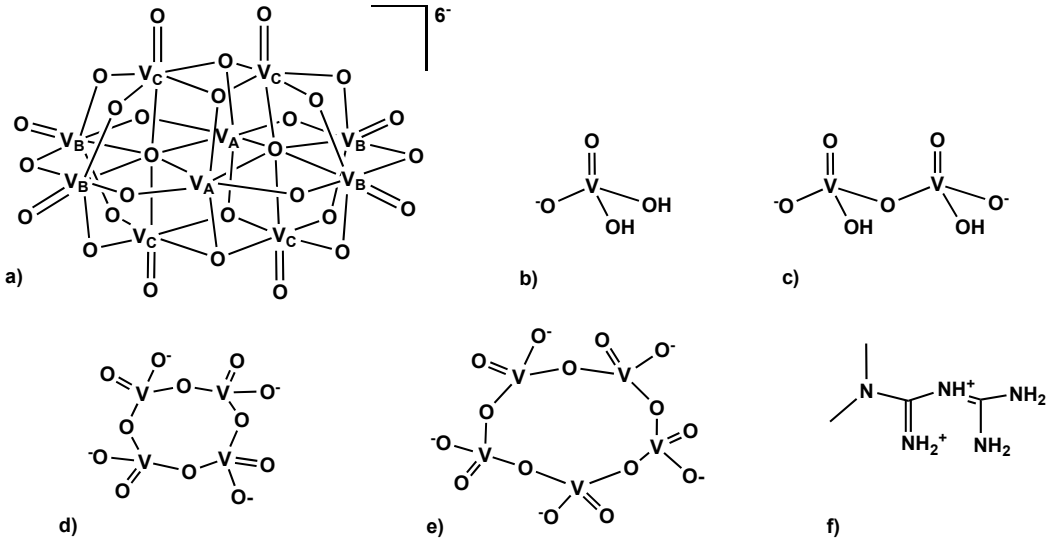

Figure 1. Schematic structure of (**a**) decavanadate anion $[V_{10}O_{28}]^{6-}$, (**b**) orthovanadate $[H_2VO_4]^-$ (V_1), metavanadate species like (**c**) $[H_2V_2O_7]^{2-}$ (V_2), (**d**) $[V_4O_{12}]^{4-}$ (V_4), (**e**) $[V_5O_{15}]^{5-}$ (V_5) and (**f**) diprotonated metformin (Metf).

Vanadium speciation is complicated under physiological conditions, many known forms of vanadium V^{4+} and V^{5+} species have been shown to readily interconvert through redox and hydrolytic reactions, and it is, therefore, difficult to determine which are the active species [18]. Additionally, in biological studies, the active vanadium species will depend on the sample preparation and handling, that is, whether the compounds were dissolved in media or buffer before addition to the cell culture and for how long the complexes have been in solution before adding aliquots to the medium [19].

Metabolic diseases like diabetes mellitus type 2 (DM2) and cancer are non-communicable diseases (NCD) that have become one of the major health hazards of the modern world [20]. Carcinogenesis occurs when normal cells receive genetic "hits", after which a full neoplastic phenotype of growth, invasion, and metastasis develops. Diabetes may influence this process through chronic inflammation, endogenous or exogenous hyperinsulinemia, or hyperglycemia, but potential biologic links between the two diseases are incompletely understood [21]. The development of innovative therapeutic modalities [22] that increase the effectiveness of clinical drugs like *cis*-platin or metformin hydrochloride and arrest their chemoresistance or side effects is a topic trend for scientists. In this context, AMP-activated kinase (AMPK) signaling has become a promising therapeutic target in hepatocellular

carcinoma [23]. Another interesting target is the identification of exploitable vulnerabilities for the treatment of hyperactive phosphatidylinositol 3-kinase (PI3K/AKT) tumors [24], and combining inhibitors of the pentose phosphate pathway (PPP) may represent a promising approach for selectively causing oxidative stress-induced cell killing in ovarian and lung cancer cells [25].

The medicinal potentiality of vanadium compounds is a challenging task that demands investigation [26] and in general few groups have pursued it. The insulin-like effects of vanadium have been tested in vitro and in vivo [27,28]; however, the applied necessary dose of vanadium still was close to the levels at which side effects are observed [29]. In fact, there is only one vanadium compound that has been tested in humans, the bis(ethylmaltolato)oxovanadium(IV) (BEOV). In general, 20 mg of vanadium compound was well tolerated [30], but at the end of Phase IIa clinical trial, the trial was abandoned due to renal problems of some patients [31]. However, several questions about the transport and mode of action of the vanadium compounds need to be addressed [28] due to the distinct action mechanism that regulates glucose metabolism by vanadium [32].

In this work, we have studied the kinetics of the decomposition of 0.5 and 1 mM sodium decavanadate (NaDeca) and metforminium decavanadate (MetfDeca) in Dulbecco's modified Eagle's medium (DMEM) solution at pH 7.4 by ^{51}V NMR, with the aim to understand the medium and the vanadium concentration effects in both, the decomposition rate and the influence in the ratio of the final products, namely V_1, V_2, V_4 and V_5. To our knowledge, the ammonium decavanadate compound decomposition in MES; MES = 2-(*N*-morpholino)ethanesulfonic acid by ^{51}V NMR is the only report that describes the decomposition reaction [14]. Thus, NaDeca stability has not been extensively studied in buffer solutions. NaDeca and MetfDeca compounds are composed of the highly negative charged decavanadate and the positive counter ions. The counter ions bonding with the decameric moiety are ionic [33]. In that regard, the same biological activity of both compounds was expected if metformin hydrochloride (Metf) was pharmacologically an inactive molecule. Nevertheless, due to Metf antidiabetic properties, different results were expected in the biological activity of the NaDeca and MetfDeca compounds. MetfDeca compound in vivo exhibited hypoglycemic and lipid-lowering properties in type 1 diabetes mellitus (T1DM) [34] and type 2 diabetes mellitus (T2DM) models [35]. However, some questions were not addressed in those studies, like if MetV and MetfDeca regulated hyperglycemia and oxidative stress with the same action mechanisms, MetfDeca stability and toxicological effects [35].

With the aim to address some of the former questions and to estimate if two different counter ions could play a role as activators or inhibitors in the biological activity of decavanadates, we investigated how the decomposition products in DMEM medium at pH 7.4 can promote damage on the cell viability of HEK293 human embryonic kidney cells and HEPG2 human liver cancer cells. A comparison of these results with the cytotoxic effect of sodium orthovanadate and metformin hydrochloride was also performed. In addition, the activation of AKT and AMPK pathways for the HEPG2 cell line by the vanadium compounds were studied in order to establish if the hydrolysis products promote the same activation mechanism in the metabolic pathways. Finally, glucose uptake in 3T3L-1 differentiated adipocytes study is presented along with an insulin release assay in βTC-6 cells at 30 μM concentration of the vanadium compounds, with the purpose of identifying if the same active species are promoting the desirable effects in each case.

2. Results and Discussion

2.1. Characterization of the Sodium and Metforminium Decavanadate Solutions

The metforminium decavanadate (MetfDeca) $(C_4H_{13}N_5)_3V_{10}O_{28}{\cdot}8H_2O$ and the sodium decavanadate (NaDeca) $Na_6V_{10}O_{28}{\cdot}18H_2O$ were prepared according to previously reported procedures [33,36].

The ^{51}V NMR spectra for 1 mM concentration of NaDeca and MetfDeca compounds were recorded at pH 4 in 10% DMSO-*d*6 and 90% H_2O (*v*/*v*), showing three signals at −420, −494, −510 ppm that were assigned to decameric species $[V_{10}O_{28}]^{6-}$ (V_{10}), attributed to the three different vanadium atoms of the

decavanadate structure V_{10A}, V_{10B} and V_{10C} respectively and one signal at −556 ppm assigned to the diprotonated monomeric species $[H_2VO_4]^-$ (V_1) (Figure 2a) [37]. The ^{51}V NMR spectra for both 0.5 and 1.0 mM concentration samples for NaDeca and MetfDeca complexes show the same species present in the solution; additionally, the complexes are stable through time. These results are in agreement with the reported V_{10A}, V_{10B} and V_{10C} peaks that were observed for 10 mM NaDeca solution in D_2O at pH 3.1 and in Middlebrook 7H9 broth medium supplemented with 10% ADC enrichment (5% BSA, 2% dextrose, 5% catalase), glycerol (0.2%, *v*/*v*) and Tween-80 (0.05%, *v*/*v*) at pH 6.5. [13] In contrast, NaDeca and MetfDeca are not stable in the DMEM medium at pH 7. Their hydrolysis products are orthovanadate $[H_2VO_4]^-$ (V_1) and metavanadate species like $[H_2V_2O_7]^{2-}$ (V_2), $[V_4O_{12}]^{4-}$ (V_4) and $[V_5O_{15}]^{5-}$ (V_5) that are observed at −556, −570, −578 and −586 ppm, respectively (Figure 2b) like previously reported for 1 mM solution of $(NH_4)_6$ $[V_{10}O_{28}]\cdot 6H_2O$ in MES buffer (0.1 M), NaCl (0.5 M) at pH 8 [14].

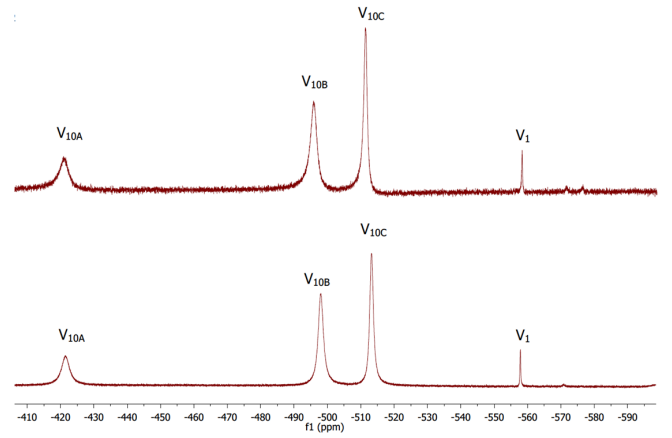

(**a**)

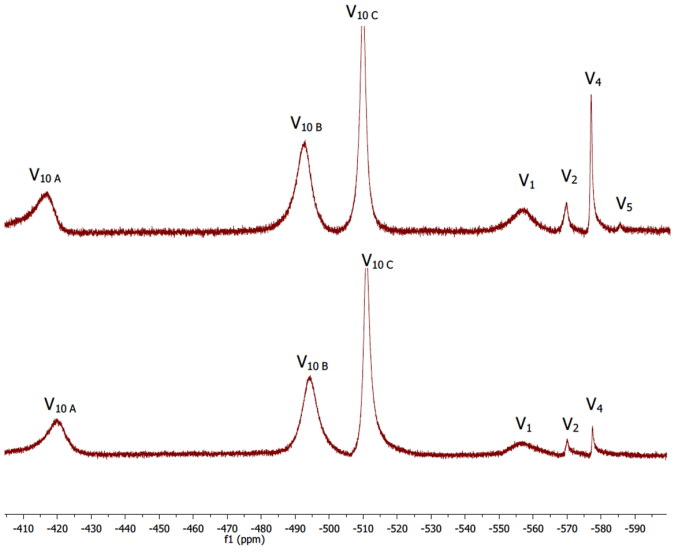

(**b**)

Figure 2. ^{51}V NMR spectra of (**a**) 1 mM NaDeca (top) and MetfDeca (bottom) in 10% DMSO-*d6* and 90% H_2O (*v*/*v*) DMSO at pH 4, (**b**) 1 mM NaDeca (top) and MetfDeca (bottom) in DMEM medium at pH 7.4.

2.2. *Kinetic Studies by ^{51}V NMR*

In vanadium(V) solutions, different oligomeric vanadate species can occur simultaneously, depends on several factors such as vanadate concentration, pH and ionic strength [12], so at 0.5 and

1 mM of NaDeca and MetfDeca, the V_{10} and V_1 species were present at pH 4, but the hydrolysis of both compounds in DMEM medium allowed us to follow by ^{51}V NMR the formation and the increment in the concentration over time at 25 °C of the orthovanadate, V_1 and metavanadate species V_2, V_4 and V_5 at −556, −570, −578 and −586 ppm, respectively. The kinetics of the decomposition of 1.0 mM NaDeca and MetfDeca (10 mM total vanadium) are plotted in Figure 3a, where the vanadium concentration for V_{10} species was calculated by integration of the V_{10A} (2 vanadium atoms), V_{10B} (4 vanadium atoms) and V_{10C} (4 vanadium atoms) resonances at −420, −494 and −510 ppm, respectively, and the rate constants for the three decavanadate signals V_A, V_B and V_C are shown with a negative sign by convention in Table 1. For comparison, the increase in concentration of the V_1 and V_4 vanadate species as a function of time are plotted in Figure 3b. Interestingly, the reaction is faster at 0.5 mM concentration of decavanadate than at 1 mM for NaDeca and MetfDeca compounds (Table 1). The rate constants of 0.5 mM NaDeca $(2.28 \pm 0.08) \times 10^{-3}$ and $(1.72 \pm 0.07) \times 10^{-4}$ for the appearance of V_4 and V_5 species, respectively, are three and four times higher than the ones calculated for 0.5 mM MetfDeca compound $(7.63 \pm 0.8) \times 10^{-4}$ and $(4.09 \pm 0.3) \times 10^{-5}$ for V_4 and V_5 species, respectively. Surprisingly, the rate constants for the appearance of the V_4 and V_5 species (Table 1) do not differ significantly for 1 mM NaDeca compared with 1 mM MetfDeca.

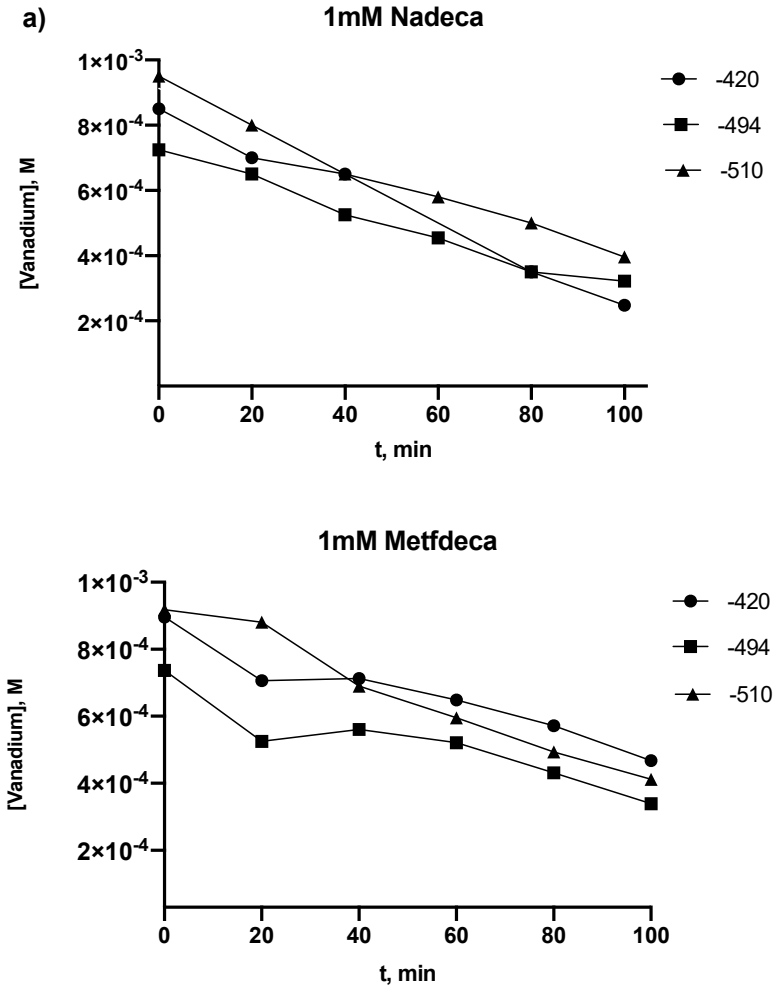

Figure 3. *Cont.*

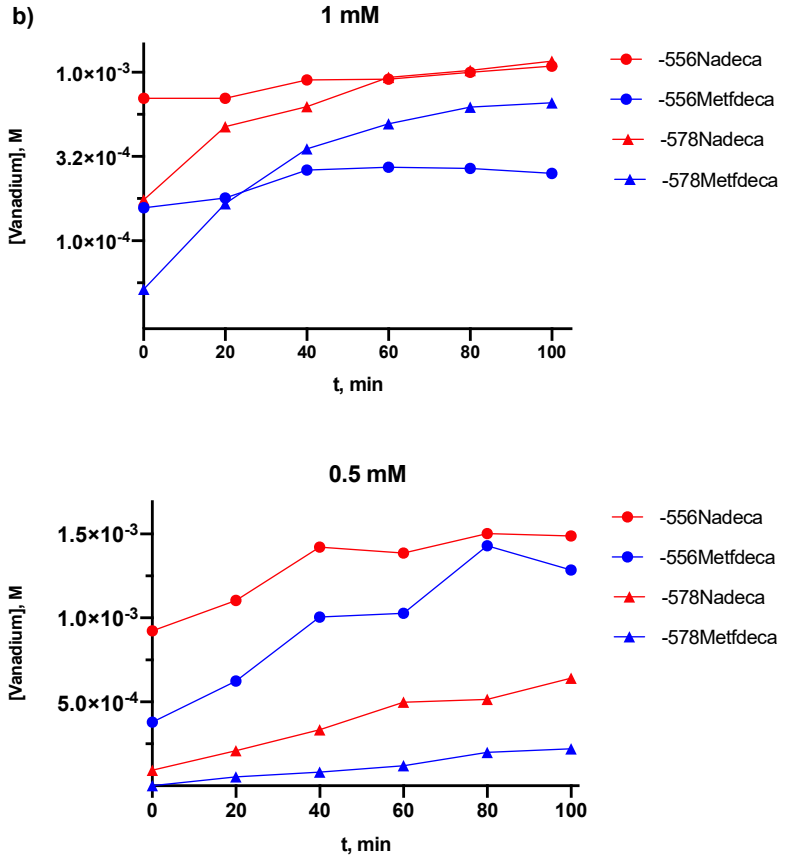

Figure 3. (**a**) ^{51}V NMR decomposition of 1 mM NaDeca and MetfDeca in Dulbecco's modified Eagle's medium (DMEM) medium, plotted as vanadium concentration (10 mM total vanadium concentration) associated with the decameric species V_{10A} (circle), V_{10B} (square), V_{10C} (triangle) over time at 25 °C. (**b**) Hydrolysis of (left) 1 mM and (right) 0.5 mM NaDeca and MetfDeca in DMEM medium followed by the formation of the orthovanadate V_1 at −556 ppm (red circle for NaDeca and blue circle for MetfDeca) and metavanadate species V_4 at −578 ppm (red triangle for NaDeca and blue triangle for MetfDeca) over time at 25 °C.

The decomposition of NaDeca and MetfDeca show first-order dependence versus time. In the case of NaDeca at 0.5 and 1 mM concentration, the calculated half-life time of the decomposition in DMEM medium at 25 °C is 9 h. In contrast, the calculated lifetime for MetfDeca is 9 h and 11 h for 0.5 mM and 1 mM concentration, respectively (Table 1). These results are in line with the half-life time for the decomposition of decameric species found by Ramos et al., where for 10 μM decavanadate concentration in different buffers pH 7–7.5, the half-life time is between 5 to 10 h. In that study, the authors performed a stabilization study of the decavanadate species with the G-actin protein, and due to the coordination of the protein with the decameric species, its half-life time was increased five times from 5 to 27 h at 10 μM of decavanadate concentration, however, in the same study the addition of 200 μM of ATP to the medium prevented the actin polymerization by V_{10} and the half-life time decreased from 27 to 10 h [12].

The decomposition rate of the decavanadate moiety is sensitive to the cations present in solution [16], the fast reaction in acid media can be accelerated by alkali metal cations and slowed down by large cations such as tetra-alkylammonium ions due to the formation of ionic-pairs with the protonated decavanadate to form $[VO_2]^+$ in seconds [16]. In basic media, the reaction is slower than in acid media, but the decomposition reaction proceeds via base independent (k_1') and base dependent (k_2) paths (Equation (1)). In the absence of sodium ions, the rate of reaction is independent of $[OH^-]$ [17]. In this work, it seems that the base-dependent decomposition path is active as well, because for

NaDeca and MetfDeca, the observed rate of decomposition is not increasing with decavanadate concentration in both cases (Table 1), and the presence of a high sodium concentration in the DMEM media (μ = 0.1 M NaCl), produces an increase in the decomposition rate via a reactive alkali-metal decavanadate species (k_2) Equation (1) [17,38].

Table 1. Summary of rate constants for the decomposition of 0.5 and 1.0 mM NaDeca and MetfDeca compound hydrolysis in DMEM medium at 25 °C and pH 7.4.

Decavanadate Compound Concentration	^{51}V NMR Signal [a]	k_{obs}, min^{-1} NaDeca	k_{obs}, min^{-1} MetfDeca
0.0005 M	−420 (V_{10A})	$(-1.25 \pm 0.03) \times 10^{-3}$	$(-1.40 \pm 0.03) \times 10^{-3}$
	−494 (V_{10B})	$(-1.26 \pm 0.2) \times 10^{-3}$	$(-1.48 \pm 0.7) \times 10^{-3}$
	−510 (V_{10c})	$(-1.82 \pm 0.4) \times 10^{-3}$	$(-1.44 \pm 0.4) \times 10^{-3}$
	−556 (V_1)	$(4.59 \pm 0.7) \times 10^{-3}$	$(2.97 \pm 0.4) \times 10^{-3}$
	−570 (V_2)	$(7.07 \pm 0.7) \times 10^{-4}$	$(6.17 \pm 0.8) \times 10^{-4}$
	−578 (V_4)	$(2.28 \pm 0.08) \times 10^{-3}$	$(7.63 \pm 0.8) \times 10^{-4}$
	−586 (V_5)	$(1.72 \pm 0.07) \times 10^{-4}$	$(4.09 \pm 0.3) \times 10^{-5}$
0.001 M	−420 (V_{10A})	$(-1.46 \pm 0.7) \times 10^{-3}$	$(-1.36 \pm 0.2) \times 10^{-3}$
	−494 (V_{10B})	$(-1.13 \pm 0.1) \times 10^{-3}$	$(-8.39 \pm 0.2) \times 10^{-4}$
	−510 (V_{10c})	$(-1.16 \pm 0.2) \times 10^{-3}$	$(-9.49 \pm 0.5) \times 10^{-4}$
	−556 (V_1)	$(2.62 \pm 0.6) \times 10^{-3}$	$(2.00 \pm 0.2) \times 10^{-3}$
	−570 (V_2)	$(6.81 \pm 0.4) \times 10^{-4}$	$(5.34 \pm 0.4) \times 10^{-4}$
	−578 (V_4)	$(1.96 \pm 0.2) \times 10^{-3}$	$(1.85 \pm 0.09) \times 10^{-3}$
	−586 (V_5)	$(1.89 \pm 0.1) \times 10^{-4}$	$(1.38 \pm 0.8) \times 10^{-4}$

[a] For calculating the rate of consumption of the decavanadate complexes, three different resonances were used, −420, −494 and −510, whereas for calculating the rate of appearance for the V_1, V_2, V_4 and V_5, only one resonance was used.

$$-d[V_{10}O_{28}{}^{6-}]_{tot}/dt = [k_{1'} + k_2[OH^-]][V_{10}O_{28}{}^{6-}]_{tot} \quad (1)$$

$$d[V_4O_{12}{}^{4-}]/dt = [k_{1'} + k_2[OH^-]][V_{10}O_{28}{}^{6-}]_{tot} \quad (2)$$

Goddard and Druskovich's [17,38] decomposition experiments were followed by UV-Vis techniques, although metavanadate species formation was not reported. Decavanadate ^{51}V NMR signals are wide, and the spectrum acquisition takes longer than the UV-Vis one. However, metavanadate species formation can be followed by ^{51}V NMR. In Table 1, NaDeca hydrolysis products formation rates are moderately faster than the ones calculated for MetfDeca, and the reaction rate is not increasing with the decavanadate concentration, so Equation (1) for the decomposition reaction was rewritten as Equation (2), where the reaction rate was expressed in terms of the metavanadate species formation. Based on the literature and our results, we proposed that in high alkali metal concentration, like in DMEM medium, the sodium ions form an ionic aggregate with the V_{10} species (Scheme 1), which then reacts with the hydroxide ion [17]. In this work, M^+ is the sodium ion, and the M′ is the metformin cation ($C_4H_{12}N_5{}^+$), which at pH 7 is monoprotonated [33].

$$[(C_4H_{12}N_5)V_{10}O_{28}]^{5-} + Na^+ \overset{K_{1P}}{\rightleftharpoons} [NaV_{10}O_{28}]^{5-} + (C_4H_{12}N_5)^+$$

$$[NaV_{10}O_{28}]^{5-} + Na^+ \overset{K'}{\rightleftharpoons} [Na_2V_{10}O_{28}]^{4-}$$

$$[Na_2V_{10}O_{28}]^{4-} + OH^- \xrightarrow{k_2{}^M} PRODUCTS$$

Scheme 1. Putative reaction mechanism for decavanadate decomposition reaction in DMEM medium at pH 7.4.

The base dependent equation can be rewritten as:

$$Rate = k_2[OH^-][V_{10}O_{28}{}^{6-}]_{tot} = k_2{}^M[OH^-][V_{10}O_{28}{}^{6-}]_{tot} \quad (3)$$

where

$$[V_{10}O_{28}{}^{6-}]_{tot} = [(C_4H_{12}N_5)V_{10}O_{28}{}^{5-}] + [NaV_{10}O_{28}{}^{5-}] + [Na_2V_{10}O_{28}{}^{4-}] \quad (4)$$

In DMEM medium, it seems likely that the ion-pair association is stronger with the metformin cation $(C_4H_{12}N_5)V_{10}O_{28}^{5-}$ at 1 mM MetfDeca concentration, which does not form at the same rate as the $Na_2V_{10}O_{28}^{4-}$ active species to react with the free OH^- anion (Scheme 1) like 1 mM NaDeca, where the total V_{10} anion concentration (Equation (4)) is almost in the higher ionic aggregate $Na_2V_{10}O_{28}^{4-}$ species, and on that way can follow the base-dependent path (Equation (3)). However, the same calculated values for the decomposition rate of 0.5 mM and 1 mM NaDeca (Table 1) suggest that the concentration of $Na_2V_{10}O_{28}^{4-}$ species remains the same under the buffer conditions; several ion-pairs can be proposed by the combination of monovalent cation and hexavalent anion. Nevertheless, Schwarzenbach and Geier [39] showed that the alkali metal cations formed the ion-pair complexes $MHV_{10}O_{28}^{4-}$, $MV_{10}O_{28}^{5-}$, and $M_2V_{10}O_{28}^{4-}$ base on their formation constants 91% of the decavanadate is in the ion-pair form $M_2V_{10}O_{28}^{4-}$ and 9% in the form $MV_{10}O_{28}^{5-}$ for M = Li or Na [39].

In vanadium speciation diagrams, at total vanadium concentration lower than 5 μM, the decavanadate anion is not formed [10], but some meta and orthovanadate species are present in solution at neutral pH. In that regard, this kinetic study was performed to have an approximate of the constant rate values at which the oligomer vanadium species were formed and, with some cautions in the interpretations of the data, would allow us to compare the biological activity of MetV (V_1) and Metf versus NaDeca and MetfDeca to show if the hydrolysis products produce a different biological response than the orthovanadate (V_1) and to quantify if MetfDeca compound promotes a synergistic effect between its components that increase the decavanadate antidiabetic properties. In that regard, the biological experiments that are shown in the next sections were performed in DMEM solution at pH 7.4, and the cells were incubated with the compounds for 24 h, with the exception of the insulin release assay, where the cells were incubated with the compounds for one hour.

2.3. Cell Viability

To investigate the cytotoxicity of vanadium compounds against non-tumoral and tumoral human cells and potential anticancer activity, the compounds NaDeca, MetfDeca, MetV and Metf were tested against HEK293 human embryonic kidney cells and HEPG2 human liver cancer cells. In Figure 4a, the percentage of cell viability vs. compound concentration for the four compounds against HEK293 is shown. The IC_{50} value found for NaDeca was 40 ± 4 μM, for MetfDeca was 85 ± 5 μM, for sodium MetV was 181 ± 7 μM and for Metf was 420 ± 11 μM. In the case of the HEPG2, the cytotoxicity dose dependence is shown in Figure 4b. The highest cytotoxic activity was observed for NaDeca, with an IC_{50} value of 9.0 ± 0.7 μM, follow by the MetfDeca with an IC_{50} of 29 ± 0.7 μM, and IC_{50} values of 93 ± 5 and 540 ± 4 μM for MetV and Metf, respectively.

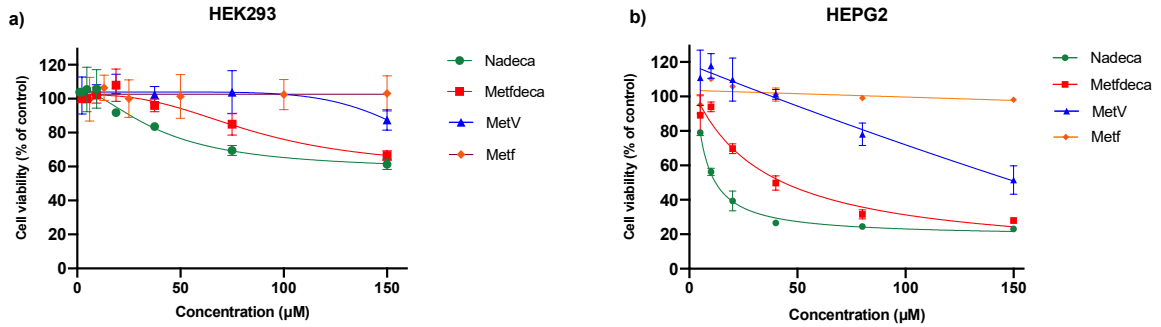

Figure 4. Cell viability assay at different vanadium compounds concentrations after treatment for 24 h (**a**) HEK293 and (**b**) HEPG2 cells. The cell viability of each treatment group was compared with the corresponding untreated control, which was normalized to 100% of cell viability. Error bars represent the standard deviation for triplicate runs (n = 3).

As can be seen in Figure 4a,b, the cell viability decreases in a dose manner response. The IC_{50} of the vanadium compounds against HEPG2 cells is around the same value as other compounds previously reported, like cis-platin (15.9 μM) [40] and monomeric V^{4+} compounds [41–43].

The metformin hydrochloride does not reduce the cellular viability in the range of concentrations that the decavanadate compounds do; the NaDeca compound exhibits more activity than MetfDeca and MetV regardless of the cell line after 24 h. The cytotoxicity of the tested compounds against HEPG2 is different for the non-tumorigenic HEK293 cells indicating that the toxicity of the compounds exhibits a good correlation on selectivity toward HEPG2 cancer cells in 24 h (see Table 2). The three vanadium and Metf compounds do not affect the viability of the HEK293 cells; this is an important result from this work, which may have an impact due to the new strategies intended to reduce the renal toxicity induced by cisplatin [44,45].

Table 2. Cytotoxic activity (IC_{50}) and selectivity index (SI) of compounds against HEK293 and HEPG2 cells after 24 h.

Compound	HEK293 Lower Cell Viability (%)	HEK293 IC_{50} (μM)	HEPG2 Lower Cell Viability (%)	HEPG2 IC_{50} (μM)	SI (IC_{50} HEK293/ (IC_{50} HEPG2)
NaDeca	61	40 ± 4	22	9 ± 0.7	4.4
MetfDeca	67	85 ± 5	28	29 ± 0.7	2.9
MetV	88	181 ± 7	51	93 ± 5	1.9
Metf	100	420 ± 11	98	540 ± 4	0.77

In the case of decavanadate compounds, the IC_{50} seems strongly dependent on the type of cell line and the counter ion; for example, the IC_{50} of the $Na_4[(HOCH_2CH_2)_3NH]_2[V_{10}O_{28}]\cdot 6H_2O$ towards HEPG2 cell line is 16.4 ± 3 μg/mL while for human cervical cancer cell line (Hela cells) is 53.1 ± 12.1 μg/mL [46], the compounds $[(H_2tmen)_3V_{10}O_{28}]\cdot 6H_2O$ and $[(H_2en)_3V_{10}O_{28}]\cdot 2H_2O$ were tested in human normal hepatocytes L02, and their IC_{50} values are 6.5 ± 0.6 and 7.2 ± 0.7 μM, respectively indicating that are cytotoxic for the L02 human cell line [47]. In 2018 Nunes and coworkers studied the cytotoxicity effect of three decavanadates compounds in African green monkey kidney (Vero) cells, and the three compounds exhibit low effect; 200 μM of the compounds reduced 50% of the Vero cells viability in 96 h. The compounds tested were the decavanadate complexes of sodium, nicotinamidium $[(3\text{-Hpca})_4H_2V_{10}O_{28}]\cdot 2H_2O\cdot 2(3\text{-pca})$ and isonicotinamidium $[(4\text{-Hpca})_4H_2V_{10}O_{28}]\cdot 2(4\text{-pca})$ [48]. However, in the three studies presented before [46–48] for decavanadate compounds, the effect of the counter ion in the cytotoxic studies was not studied.

It seems that the decavanadate compounds—or their decomposition products V_1, V_2 and V_4—decreased the viability of hepatocarcinoma HEPG2 cells faster than the normal HEK293 cells (Table 2) after 24 h. The cytotoxicity of cancer and normal cells can be attributed to a different mechanism like Wang and coworkers reported in 2010 [49] that for 100 μM of MetV in MEM (minimum essential medium) in normal hepatocytes L02, the cell arrest mechanism is ROS-dependent and for HEPG2 is ROS-independent to mediated ERK (extracellular signal-regulated protein kinase activation) after 72 h. In the present study, the Metf cation association with the decavanadate moiety promotes some kind of protection against the normal HEK293 cells. However, the dissociation of the ion-pairs $NaV_{10}O_{28}^{5-}$, $(C_4H_{12}N_5)V_{10}O_{28}^{5-}$ and the further hydrolysis to V_1 and other products will not protect the vanadium atoms for the reduction into V^{4+} that could significantly increase the ROS levels and the apoptosis for the normal cells.

2.4. Proteins Expression

Protein kinase B (AKT) is a crucial mediator of insulin-resistant glucose and lipid digestion [50]. To evaluate the effect that decavanadate compounds have in phosphatidylinositol 3-kinase (PI3K/AKT) and AMPK pathways in HEPG2 cells, a Western blot examination was performed.

The cells were cultured with various concentrations of the compounds for 24 h without insulin. In Figure 5a we can see that NaDeca highly phosphorylates AKTα while the MetfDeca, MetV and Metformin show moderate activity. Thus, NaDeca and MetfDeca compounds exhibit a dose-dependence increase in phosphorylated AKT (p-AKT) as shown in Figure 5c, where 8, 16, and 30 μM of NaDeca induced a 2, 4 and 6-fold-increase in the phosphorylation, respectively. In contrast, the expression of the AMPK, a cellular metabolism energy sensor, by its phosphorylation p-AMPKα is not significantly elevated by the compounds (Figure 5d). However, NaDeca in 8 μM concentration exhibits around 33% of the increase in the AMPK phosphorylation. The low percentage of phosphorylation in AMPK by the vanadium compounds and metformin (Figure 5d) can be explained as follows: in hepatocellular carcinoma (HCC), the pathway function is downregulated [51], it seems like a low level of AMPK is required to maintain viability during the metabolic stress of tumor cells by different mechanisms [52].

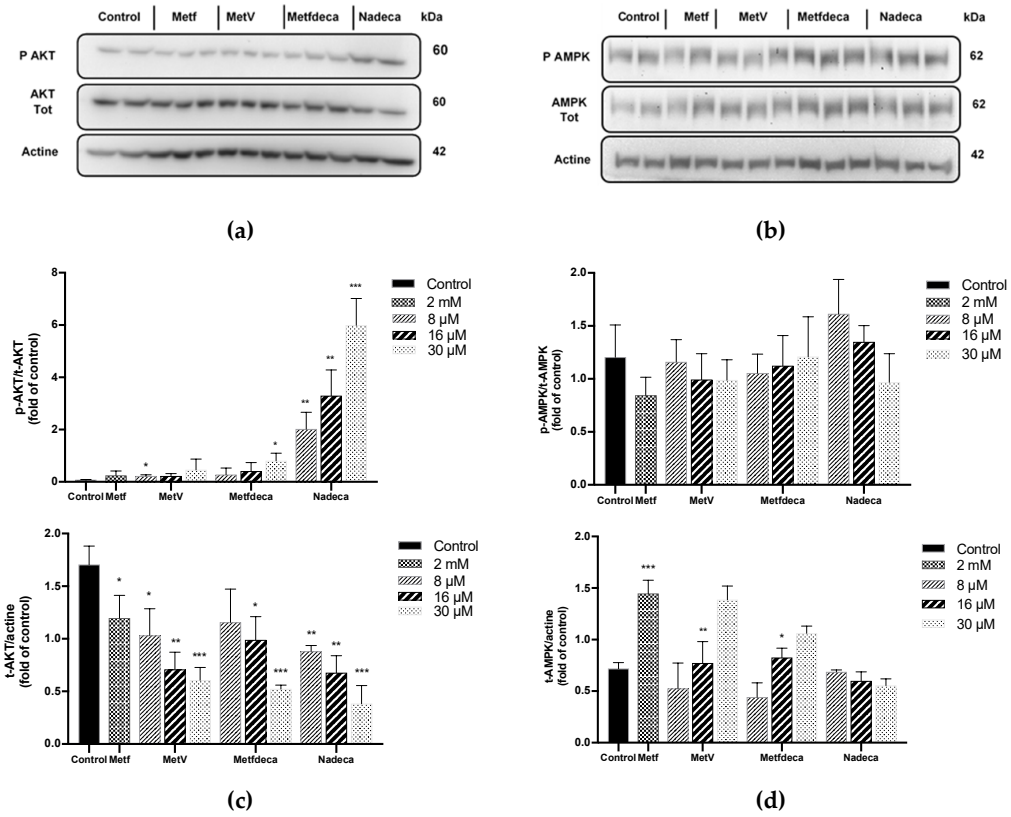

Figure 5. Effect of vanadium compounds on the protein expression of (**a**) protein kinase B (AKT) representative Western blot and (**b**) AMP-activated kinase (AMPK) representative Western blot in HEPG2 human hepatocarcinoma cells. Metf 2 mM and vanadium compounds 8, 16 and 30 μM concentrations, respectively, from left to right. Quantitative data of (**c**) p-AKT/t-AKT and t-AKT/actine (**d**) p-AMPK/t-AMPK and t-AMPK/actine. All the values are the mean ± SD. * $p < 0.05$, ** $p < 0.01$ and *** $p < 0.001$ vs. untreated control cells.

In the present work, the activation of AKT by 2 mM of Metf and by 8–30 μM of MetfDeca is moderate; in the case of Metf, p-AKT is increased by 21% while for 30 μM of MetfDeca, the increase is 80%; however, we observed that the NaDeca formation rate of metavanadate species is moderately faster than MetfDeca under the same experimental conditions (Table 1), due to the weaker ionic pairs for NaDeca than for MetfDeca (Scheme 1), so if all the 8 μM NaDeca decomposition product is V_1 the p-AKT fold should be ten times 0.21, the fold value that we found experimentally for the MetV is 2.1 (Figure 5c), this clearly indicates that 8 μM of NaDeca is decomposed to 80 μM of V_1. Nevertheless, the decomposition of NaDeca at higher concentration solutions shows lower amounts of V_1 produced, based on the p-AKT fold activity. If we double NaDeca concentration to 16 μM, the experimental fold

value is 3.3 for the decameric compound, and for MetV is 0.21, while for 30 μM of MetV, the p-AKT fold value is 0.45 and for NaDeca is 6. It seems that higher vanadium concentrations induce the formation of larger oligomers like V_2, V_4 and V_5. Thus the active species could be a combination of the orthovanadate and the metavanadate units, with differing AKT signaling activation mechanisms promoted by different vanadium species.

Activation of the IR kinases by vanadium compounds exhibit different mechanisms, which depend on the type of cell and also the oxidation state of the metal [53,54]. Recently, several lines of evidence suggest that cancer cells upregulate the oxidative pentose phosphate pathway (PPP) to support cell growth and survival, by consequence exhibited increased PPP flux, NADPH/NADPC ratio, and ROS [25], in the liver 30% of the glucose oxidation occurs via PPP, so, it is not surprising that the AKT activation could be in a phosphatidylinositol 3-kinase (PI3K)-dependent manner by ROS [24]. However, in our control experiments the AKT signal in HEPG2 cells has not been activated (Figure 5c), suggesting that AKT phosphorylation by MetV, MetfDeca and NaDeca can be attributed to the activation of PTB-1B by orthovanadate (V_1) [32]. On the other hand, for NaDeca compound, the tetramer species is formed at the same speed than V_1 (Table 1), V_4 could be the one that is reduced [55] and the vanadium (IV) species VO^{2+} is activating the AKT pathway in a PI3K-dependent manner by ROS, like in the case of $VOSO_4$ that exhibited a 17-fold increase in the phosphorylation of AKT in HEPG2 cells at 25 μM concentration [56]. In 2015 Levina and coworkers performed a speciation study by XANES spectroscopy, where for 1 mM of orthovanadate in HEPG2 cells with DMEM medium after 24 h, 50% of the initial vanadium was found as tetrahedral species of V^{5+} (V_1, V_2, V_4 and V_5 are tetrahedral), 30% as V^{4+} moieties with a coordination number of six and 20% as V^{4+} with a coordination number of five [19], this study supports our observation that after 24 h not more decavanadate species are present in solution. It also supports our hypothesis that not all the vanadium in solution is present in the highest oxidation state (V^{5+}) and some has been reduced to V^{4+} promoting different mechanism of AKT activation, particularly for the NaDeca compound.

2.5. Glucose Uptake Assay

To establish whether MetV, MetfDeca, NaDeca and Metf compounds stimulate glucose uptake on adipocytes, the effect on the 2-NDBG cell uptake in 3T3-L1 differentiated adipocytes was evaluated. The experiments were performed at 16, 30 μM concentration for vanadium compounds and 2 mM for Metf in the absence of insulin. Insulin (100 nM) was used as a positive control. As it can be seen in Figure 6, NaDeca (30 μM) stimulates the glucose cell uptake on 62%, MetfDeca on 52%, MetV on 37% and Metf (2 mM) on 33%, while control conditions stimulate around to 20%. At 16 μM, NaDeca stimulates 29% and is the only compound that shows a notable difference between both concentrations. Our results suggest that the uptake is moderate due to the low concentration of the compounds; it has been shown that elevated concentrations of decavanadate 100 μM [6] and vanadate 325 μM were required for stimulation of glucose uptake in rat adipocytes, the later associated with IR Tyr auto-phosphorylation [53]. The activation of the insulin receptor substrates (IRS) has been demonstrated to occur in a dose-dependent manner in cardiomyocytes for MetV [54] and in 3T3-L1 cells for $VOSO_4$ [57] due to different mechanisms of actions. Our results indicate that the PI3K pathway was activated due to the activation of IRS-1 by PTPB1 phosphorylation for MetfDeca, MetV and Metf by a combination of different mechanisms that includes PTPB1 phosphorylation, and for NaDeca by a ROS production, where V_1 and the metavanadate species are involved, the ROS production by a decavanadate compound and the activation of the semicarbazide-sensitive amine oxidase (SSAO)/vascular adhesion protein-1 (VAP-1) was reported by Ybarola [58] the compound hexakis(benzylammonium) decavanadate showed that can stimulate glucose uptake in rat adipocytes in a dose dependent manner EC_{50} 150 μM, an in vitro assay they confirmed that hexakis(benzylammonium) decavanadate is oxidized in the same extension by SSAO enzyme as benzylamine and vanadate, using ^{51}V NMR the authors also found that for 10 mM of the compound in the presence of 2.5 mM of H_2O_2 at pH 7.4, the major products of the decavanadate decomposition were V_1, V_4 and $[V(OH)_2(OO)_2(OH)_2]^{2-}$. The decomposition products promoted the

inhibition of PTP and the activation of SSAO that regulates the translocation of the GLUT4 transport and stimulates glucose transport [58], like in the case of the vanadium compounds tested in this work, where the GLUT4 transport is translocated and the glucose is transported by the cell.

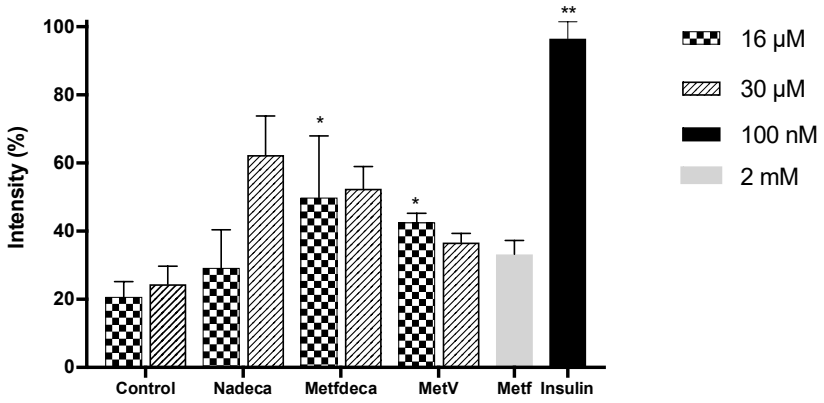

Figure 6. Effect of vanadium compounds on the glucose uptake in 3T3-L1 differentiated adipocytes at 16, 30 µM for vanadium compounds and 2 mM for Metf in the absence of insulin. All the values are the mean ± SD. * $p < 0.05$ and ** $p < 0.01$ vs. untreated control cells.

2.6. Insulin Release Assay

The effect on insulin release of NaDeca, MetfDeca, MetV at 30 µM concentration was studied in βTC-6 cells. Glucose 10 mM and repaglinide 30 µM concentration were used as control. The latter was used due to the pharmacological activity, such as blocking ATP-dependent K^+ channels and stimulate the release of insulin from the pancreas in a dose-dependent manner [59]. Figure 7 shows that MetV and MetfDeca enhanced insulin release by 0.7 and 1-fold relative to glucose control. In addition, both vanadium compounds showed more activity than the repaglinide at the same concentration, while NaDeca shows lower activity at 30 µM concentration than the glucose and repaglinide controls. βTC-6 cells secrete insulin in response to glucose; however, this cell line derived from transgenic mice develop a high hexokinase activity [60]; in normal pancreatic β-cells isolated from mouse islets, the effects of $NaVO_3$ were studied at 0.1–1 mM concentration [61], the authors found that vanadate did not affect basal insulin release, although, vanadate potentiated the glucose effect by a different mechanism than blocking the sodium pump or affecting the AmpC levels [61].

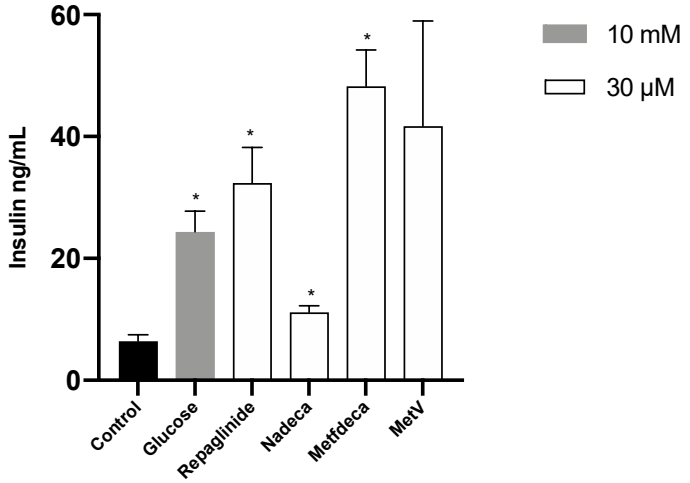

Figure 7. Effect of the vanadium compounds (30 µM concentration) on the insulin release in βTC-6 cells with 10 mM of glucose and 30 µM of repaglinide. All the values are the mean ± SD. * $p < 0.05$ vs. untreated control cells.

In 1999, Proks and coworkers performed an experiment in different types of cloned K_{ATP} channels expressed in *Xenopus oocytes* [62]. Their results showed that sodium decavanadate in 2 mM concentration made by a solution of Na_3VO_4 at pH 7.2 modulated K_{ATP} channel activity via the SUR subunit, the Hill coefficients for both activation and inhibition of K_{ATP} currents suggested that the cooperativity action of more than one vanadate molecule was involved in these effects. They also found that the effects were abolished by boiling the solution where the vanadate polymers where virtually absent [62]. Our results indicate that vanadium species promote more than one insulin release mechanism in βTC-6 cells (Figure 8), MetV, NaDeca, and MetfDeca decomposition in V_1 augment insulin secretion by tyrosine phosphorylation of IRS-1 and IRS-2 [63,64], while in the second mechanism, vanadium oligomers can be active blocking ATP-dependent K^+ channels, however, we propose that the active species in the decavanadate solutions are the vanadium dimers V_2, although, V_2 formation rate is slower (Table 1), it can be present in considerable amounts blocking ATP-dependent K^+ channels [62,65]. In the case of V_4, the higher oligomer formation is promoted by the decomposition reaction of the NaDeca compound (Table 1), and the tetramer V_4 has not followed any of the two mechanisms (Figure 8). It has been shown that vanadium compounds like $VOSO_4$ and $NaVO_3$ (1.6–100 μM) stimulated ROS production in isolated rat liver mitochondria [66]. In 2013 Hosseini and coworkers showed that V^{5+} (25–200 μM) interaction with respiratory complex III is the major source of V^{5+} induced ROS in rat liver mitochondria [67]. Interestingly, the concentration of ROS formation highly increases with 200 μM of sodium metavanadate in 60 min while with just 50 μM, it is not the case [67]. We hypothesized that NaDeca at 30 μM concentration product V_4 has some interaction with the cell mitochondria like its membrane depolarization [68] through ROS production that inhibits the insulin release by NaDeca compound.

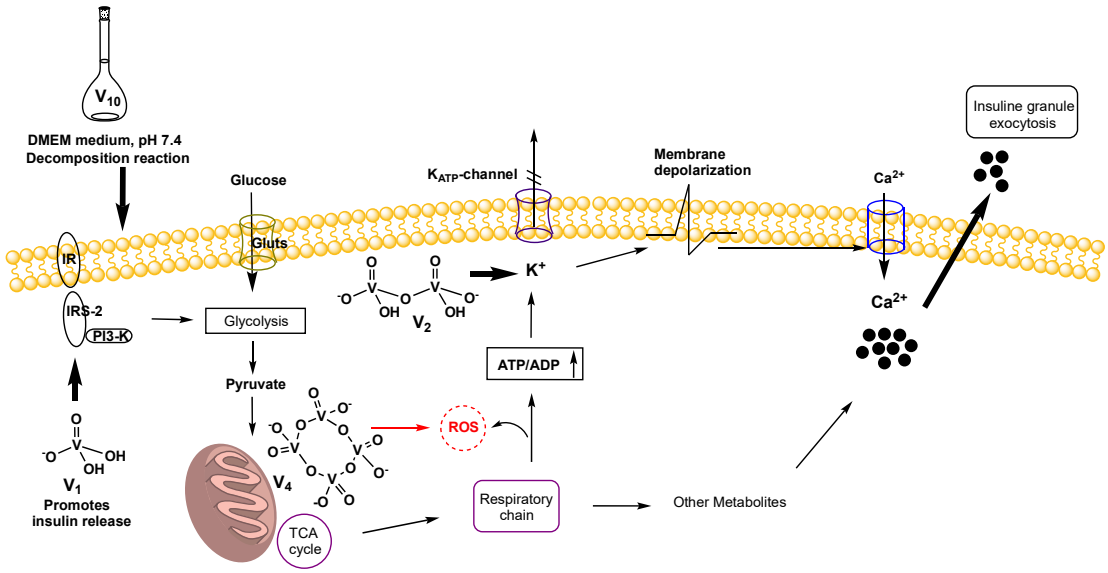

Figure 8. Illustration of the vanadium species mechanisms of action on the insulin release in βTC-6 cells. The total vanadium concentration is 300 μM, NaDeca decomposition reaction is moderately faster than MetfDeca reaction (Table 1), so NaDeca and MetfDeca majority decomposition products are V_1 and V_4; however, some V_2 is present, the putative mechanism of action for V_1 is that enhanced tyrosine phosphorylation, and on that way, V_1 species is able to further augment insulin secretion. A second putative mechanism involves inhibition of the K_{ATP} channel by V_2 species.

3. Experimental

3.1. Chemicals and Reagents

Ammonium metavanadate (NH_4VO_3), sodium metavanadate ($NaVO_3$), hydrochloric acid (HCl 37% *w/v* in H_2O), dimethyl sulfoxide (DMSO), *d*6-DMSO, deuterium oxide (D_2O), 3-(4,5-dimethylthiazol-2-yl)

-2,5-diphenyltetrazolium Bromide (MTT) 98%, 4-(2-hydroxyethyl)-1-piperazineethanesulfonic acid (HEPES), potassium chloride (KCl), sodium chloride (NaCl), ethylenediaminetetraacetic acid disodium salt (EDTA), ethylene glycol-bis(2-aminoethylether)-*N*,*N*,*N*′,*N*′-tetraacetic acid (EGTA), β-glycerol-phosphate, triton X-100, NaF, sodium pyrophosphate dibasic, sodium orthovanadate (Na_3VO_4) and 1,4-dithiothreitol (DDT) were purchased from Sigma-Aldrich (St Louis, MO, USA). Phenylmethylsulfonyl fluoride (PMSF) from Calbiochem (San Diego, CA, USA). COMPLETE (protease inhibitor cocktail) from ROCHE (Mannheim, Germany). Dulbecco's modified Eagle's medium (DMEM) high glucose, fetal bovine serum (FBS) and penicillin/streptomycin from Gibco (Gaithersburg, MD, USA). All the cell lines used were purchased from ATCC (HEP-G2 HB-8065, 3T3-L1 CL-173, Beta-TC-6 RL 11506) (Manassas, VA, USA).

Metformin hydrochloride ($C_4H_{11}N_5{\cdot}HCl$) was isolated directly from commercial brand tablets. The metforminium decavanadate (MetfDeca) $(C_4H_{13}N_5)_3V_{10}O_{28}{\cdot}8H_2O$ was prepared according to the literature [33]. The sodium decavanadate (NaDeca) $Na_6V_{10}O_{28}{\cdot}18H_2O$ was prepared by suspending $NaVO_3$ (0.12 g, 1 mmol) in distilled water (30 mL). After the suspension was stirred at room temperature for 1 h, the pH was adjusted to 4 by the addition of HCl (1 M). The resulting orange solution was filtered, and the filtrate was allowed to evaporate at 4 °C. Orange crystals were obtained after one week, according to a previously reported procedure [36].

The concentrations of the stock solutions for the biological studies in water for metformin hydrochloride (Metf), sodium metavanadate (MetV), metforminium decavanadate (MetfDeca) were 30 mM, whereas for sodium decavanadate (NaDeca) was 15 mM. The metforminium decavanadate crystals are water-insoluble, so it was solubilized in 10% DMSO before the addition of water. For the ^{51}V NMR studies, 10% DMSO-*d*6 was used.

3.2. Kinetic Studies

The kinetics of the decomposition reaction of sodium and metforminium decavanadates in DMEM medium at 25 °C was determined by ^{51}V NMR at 0.5 and 1.0 mM of decavanadate concentration. The spectra were acquired using 0.5 mL as a final volume with 10% DMSO-*d*6 in a Bruker Ascend 600 MHz spectrometer. ^{51}V spectra were recorded using parameters reported previously [12,69] at 157.85 MHz. The chemical shifts were obtained using an external reference using 100 mM Na_3VO_4 solution in 1.0 M NaOH ($[VO_4]^{3-}$ signal at −541 ppm) [70]. The concentrations of each vanadate species V_x were calculated from the fractions of the total integrated areas using the following equation: $[V_x] = (A_x/A_t) \times ([V_t]/n)$, where A_x corresponds to the area measured for the x vanadate species with n as the oligomer number (number of vanadium atoms), A_t is the sum of the measured areas and $[V_t]$ is the total vanadate concentration [71]. In the case of the decameric species, three signals at −420, −494 and −510 ppm were integrated for 2, 4 and 4 vanadium atoms, respectively [72].

The rate constants were calculated by the initial rates method, where the species concentration V_x was plotted over time (100 min), the ^{51}V NMR spectra were acquired every 20 min, and the reaction was started when the decavanadate compound aliquot was added to the DMEM medium.

3.3. Cell Viability Assay

Cell viability of the three vanadium compounds NaDeca, MetfDeca, MetV and metformin hydrochloride against HEPG2 and HEK293 was tested using MTT assay (Sigma-Aldrich, St Louis, MO, USA). The cells were placed in a 96-well micro-assay culture plate (ULTRACRUZ, Santa Cruz Dallas, TX, USA) at a density of 1×10^5 cells per well in 0.2 mL of DMEM-high glucose culture medium supplemented with fetal bovine serum FBS (10%) and penicillin/streptomycin (1%), and grown at 37 °C in a humidified 5% CO_2 incubator for 24 h. After this, the cells were treated with 0.002 mL of each compound per well by triplicate; sequential dilutions 1:2 were made for each compound, DMSO was used as a blank. The cells were incubated for 24 h. The surviving cells were determined. We added 0.01 mL of MTT (5 mg/mL in phosphate-buffered saline) to each well, and the cells were incubated for 3 h at 37 °C in a humidified 5% CO_2 incubator. After this time, the medium was removed from the cells, and 0.1 mL of DMSO was added to each well, and the cells were incubated for 1 h. The cells

viability was determined by measure their ability to reduce MTT (yellow) to formazan product (violet). The absorbance was quantified at 600 nm by a Modulus microplate Luminometer spectrophotometer (Turner BioSystems, Sunnyvale, CA, USA).

3.4. Western Blot Analysis

The cells were placed in 6-well micro-assay culture plates at a density of 5×10^5 cells per well in 3 mL of DMEM-high glucose culture medium supplemented with fetal bovine serum FBS (10%) and penicillin/streptomycin (1%); the cells were treated with 8, 16 and 30 μM of each compound and the cells were grown at 37 °C in a humidified 5% CO_2 incubator for 24 h.

Cultured cells were washed with 1 mL of cold phosphate buffer solution (PBS). For AMPK assays cells were lysed by 0.25 mL of ice-cold HEPES lysis buffer: HEPES (50 mM, pH 7.4), EDTA (1 mM), EGTA (1 mM), KCl (50 mM), glycerol (5 mM), Triton X100 (0.1% *w*/*v*), NaF (50 mM), NaPPi (5 mM), Na_3VO_4 (1 mM), DDT (1 mM), PMSF (0.2 mM) and COMPLETE 1X as protease inhibitor. Homogenates were centrifuged at 16,128× *g* for 20 min at 4 °C in an Eppendorf centrifuge 5804R.

Supernatants were collected for their protein quantitation by Lowry method; 50 μg of protein were separated by 10% SDS-page and transferred to PVDF for blotting using the following antibodies (cell signaling 1:1000) anti-pAKT (Ser473), anti-p-AMPKα (Thr172), anti-AMPKα, anti-AKT (PKBα) and anti-β-actin at 4 °C overnight. Blots were visualized with HRP-conjugated goat anti-rabbit IgG or HRP-conjugated goat anti-mouse IgG at room temperature for one hour. Actin was used as loading controls for the total protein content. Proteins were visualized and quantified in a Bio-Rad ChemiDoc XRS (Bio-Rad, Hercules, CA, USA). with the Quantity One software (Version 4.5, Bio-Rad, Hercules, CA, USA).

3.5. Adipocyte Differentiation

Preadipocytes 3T3-L1 were obtained from ATCC and differentiated, as previously described [73]. Briefly, cells were grown to confluency in a 75 cm flask (CORNING) with DMEM medium supplemented with 10% calf serum (Biowest, Riverside, MO, USA) and standard temperature and CO_2 conditions (37 °C and 5% CO_2). Two days after reaching confluency, media was replaced to induce differentiation (DMEM supplemented with 10% fetal bovine serum (FBS), 1.0 μg/mL human insulin, 0.5 mM 3-isobutyl-1-methylxanthine and 1 μM dexamethasone). After 48 h, media was changed with DMEM supplemented with 10% fetal bovine serum and 1.0 μg/mL human insulin and cells were incubated for 48 h. Finally, the media was replaced with DMEM supplemented with 10% FBS for 4 days, media was refreshed every 2 days.

3.6. Glucose Uptake Assay

3T3-L1 differentiated adipocytes cells were seeded in a 96-well plate (ULTRACRUZ, Santa Cruz) 1×10^5 cells per well. The next day media was changed to starving media (DMEM without supplementation, no glucose), compounds were added at 16 and 30 μM final concentration and incubated 20 h at standard conditions. Cells were incubated with or without 100 nM insulin for 1 h. After this, 300 μM of 2-NBDG (Invitrogen by Thermo Fisher Scientific) were added to each well and incubated 20 min at 37 °C and 5% CO_2, cells were washed once with PBS, and 100 μL/well of fresh PBS were added. Fluorescence was read at 485/535 nm (Modulus Microplate Luminometer).

3.7. Insulin Release Assay

Studies were performed with βTC-6 cells. The cells were placed in 24-well micro-assay culture plates at a density of 2.5×10^5 cells per well in DMEM culture medium; the cells were incubated overnight at 37 °C in a humidified 5% CO_2 incubator. The next day medium was changed, and 10 mM glucose and 30 μM repaglinide were added as controls. Compounds were added at 30 μM final concentration and incubated for one hour at standard conditions. The insulin quantification was made with a mouse insulin ELISA kit (ALPCO, INSMS-E01, ALPCO, Salem NH, USA).

3.8. Statistical Analysis

Data were presented as mean ± SEM of three independent experiments. Statistical significance of data was analyzed by Student's *t*-test and one-way analysis of variance (ANOVA). A probability of the value of $p < 0.05$ was considered as statistically significant. Calculations and figures were made using Grad Pad Prism version 8 (GraphPad Software, San Diego, CA, USA).

4. Conclusions

Vanadium solution chemistry represents a challenge due to its complexity. However, new therapeutic approaches can be explored with decavanadate compounds in biological reaction media, vanadium therapeutic potential in different diseases like DM2, cancer, metabolic syndrome and cardiovascular diseases should be addressed. Decavanadate decomposition products like V_2 and V_4 action mechanisms in cytotoxic activity, AMPK and AKT expression still have open questions; however, V_1 is well known as a glucose uptake promoter and insulin release agent. Nevertheless, the combination of orthovanadate and methavanadate species can increase the desirable therapeutic effects of vanadium, as shown in this work.

Our results show that at least two mechanisms are promoted AKT activation by NaDeca, and MetfDeca hydrolysis products in HEPG2 cells, the first one with the orthovanadate (V_1) species involved in PTP-1B mediated AKT activation, while the second mechanism involves the activation of the AKT pathway in a PI3K-dependent manner by ROS, in this regard, we hypothesized that V_4 could be involved in a vanadium reduction process that promotes the ROS exacerbation in HEPG2 cells in DMEM medium and that ROS production results in a decrement of the cell viability in normal (HEK293) and carcinogenic cells (HEPG2).

In this sense, our results indicate that a combination of at least two mechanisms is associated with the glucose uptake in 3T3L-1 differentiated adipocytes that includes PTP-1B phosphorylation and ROS production in the case of NaDeca.

MetfDeca and MetV at 30 μM concentration enhanced insulin release in βTC-6 cells; surprisingly, the NaDeca compound is almost inactive in the assay. Our results suggest that MetfDeca decomposition products (V_1 and V_2) promote more than one insulin release mechanism in the DMEM medium. The first proposed mechanism is that V_1 augment insulin secretion by tyrosine phosphorylation of the IRS, and in a second putative mechanism, vanadium oligomers like V_2 can be active, blocking ATP-dependent K^+ channels. However, V_4 species that are produced by the decomposition reaction of NaDeca and MetfDeca are not following either mechanism.

The data presented in this paper demonstrate that decavanadate decomposition products are able to promote different biological mechanisms of action, than the ones promoted by orthovandate (MetV) and metformin hydrochloride (Metf). Thus, more chemical and biological experiments are necessary to establish the active species and their composition with the aim to explore new therapies in the treatment of some metabolic diseases.

Author Contributions: A.M.S.-N. and R.O.S.-D. performed the kinetics experiments; A.M.S.-N. and L.C. performed the biological studies; I.E.L. and O.H.-A. reviewed and edited the manuscript; I.S.-L. wrote most of the manuscript and carried out the kinetics analysis. All authors have read and agreed to the published version of the manuscript.

Funding: This research received no external funding. A.M.S.-N. and I.S.-L. would like to thank the UJAT for funding A.M.S.-N. fellowship.

Acknowledgments: We specially thanks to Boris Rodenak Kladniew to participate in the biological data analysis.

Conflicts of Interest: The authors declare no conflict of interest.

References

1. Van Rompuy, L.S.; Parac-Vogt, T.N. Interactions between polyoxometalates and biological systems: From drug design to artificial enzymes. *Curr. Opin. Biotechnol.* **2019**, *58*, 92–99. [CrossRef]
2. Čolović, M.B.; Lacković, M.; Lalatović, J.; Mougharbel, A.S.; Kortz, U.; Krstić, D.Z. Polyoxometalates in Biomedicine: Update and Overview. *Curr. Med. Chem.* **2020**, *27*, 362–379. [CrossRef]

3. Aureliano, M. Decavanadate contribution to vanadium biochemistry: In vitro and in vivo studies. *Inorg. Chim. Acta* **2014**, *420*, 4–7. [CrossRef]
4. Bijelic, A.; Rompel, A. The use of polyoxometalates in protein crystallography—An attempt to widen a well-known bottleneck. *Coord. Chem. Rev.* **2015**, *299*, 22–38. [CrossRef] [PubMed]
5. Crans, D.C.; Sánchez-Lombardo, I.; McLauchlan, C.C. Exploring Wells-Dawson Clusters Associated with the Small Ribosomal Subunit. *Front. Chem.* **2019**, *7*, 462–476. [CrossRef] [PubMed]
6. Aureliano, M.; Crans, D.C. Decavanadate ($V_{10}O_{28}^{6-}$) and oxovanadates: Oxometalates with many biological activities. *J. Inorg. Biochem.* **2009**, *103*, 536–546. [CrossRef] [PubMed]
7. Nakamura, S.; Ozeki, T. Hydrogen-bonded aggregates of protonated decavanadate anions in their tetraalkylammonium salts. *J. Chem. Soc. Dalton Trans.* **2001**, 472–480. [CrossRef]
8. Ferreira da Silva, J.L.; Fátima Minas da Piedade, M.; Teresa Duarte, M. Decavanadates: A building-block for supramolecular assemblies. *Inorg. Chim. Acta* **2003**, *356*, 222–242. [CrossRef]
9. Bošnjaković-Pavlović, N.; Prévost, J.; Spasojević-de Biré, A. Crystallographic Statistical Study of Decavanadate Anion Based-Structures: Toward a Prediction of Noncovalent Interactions. *Cryst. Growth Des.* **2011**, *11*, 3778–3789. [CrossRef]
10. Povar, I.; Spinu, O.; Zinicovscaia, I.; Pintilie, B.; Ubaldini, S. Revised Poubaix diagrams for the vanadium–water system. *J. Electrochem. Sci. Eng.* **2019**, *9*, 620. [CrossRef]
11. Kojima, T.; Antonio, M.; Ozeki, T. Solvent-Driven Association and Dissociation of the Hydrogen-Bonded Protonated Decavanadates. *J. Am. Chem. Soc.* **2011**, *133*, 7248–7251. [CrossRef] [PubMed]
12. Ramos, S.; Manuel, M.; Tiago, T.; Duarte, R.; Martins, J.; Gutiérrez-Merino, C.; Moura, J.J.G.; Aureliano, M. Decavanadate interactions with actin: Inhibition of G-actin polymerization and stabilization of decameric vanadate. *J. Inorg. Biochem.* **2006**, *100*, 1734–1743. [CrossRef] [PubMed]
13. Samart, N.; Arhouma, Z.; Kumar, S.; Murakami, H.A.; Crick, D.C.; Crans, D.C. Decavanadate Inhibits Mycobacterial Growth More Potently Than Other Oxovanadates. *Front. Chem.* **2018**, *6*. [CrossRef] [PubMed]
14. Krivosudský, L.; Roller, A.; Rompel, A. Tuning the interactions of decavanadate with thaumatin, lysozyme, proteinase K and human serum proteins by its coordination to a pentaaquacobalt(II) complex cation. *New J. Chem.* **2019**, *43*, 17863–17871. [CrossRef]
15. Soares, S.S.; Martins, H.; Duarte, R.O.; Moura, J.J.G.; Coucelo, J.; Gutiérrez-Merino, C.; Aureliano, M. Vanadium distribution, lipid peroxidation and oxidative stress markers upon decavanadate in vivo administration. *J. Inorg. Biochem.* **2007**, *101*, 80–88. [CrossRef] [PubMed]
16. Clare, B.W.; Kepert, D.L.; Watts, D.W. Acid decomposition of decavanadate: Specific salt effects. *J. Chem. Soc. Dalton Trans.* **1973**, 2481–2487. [CrossRef]
17. Druskovich, D.M.; Kepert, D.L. Base decomposition of decavanadate. *J. Chem. Soc. Dalton Trans.* **1975**, 947–951. [CrossRef]
18. Crans, D.; Rithner, C.; Theisen, L. Application of time-resolved vanadium-51 2D NMR for quantitation of kinetic exchange pathways between vanadate monomer, dimer, tetramer, and pentamer. *J. Am. Chem. Soc.* **1990**, *112*, 2901–2908. [CrossRef]
19. Levina, A.; McLeod, A.I.; Pulte, A.; Aitken, J.B.; Lay, P.A. Biotransformations of Antidiabetic Vanadium Prodrugs in Mammalian Cells and Cell Culture Media: A XANES Spectroscopic Study. *Inorg. Chem.* **2015**, *54*, 6707–6718. [CrossRef]
20. Saklayen, M.G. The Global Epidemic of the Metabolic Syndrome. *Curr. Hypertens. Rep.* **2018**, *20*, 12. [CrossRef]
21. Giovannucci, E.; Harlan, D.M.; Archer, M.C.; Bergenstal, R.M.; Gapstur, S.M.; Habel, L.A.; Pollak, M.; Regensteiner, J.G.; Yee, D. Diabetes and Cancer: A consensus report. *Diabetes Care* **2010**, *33*, 1674–1685. [CrossRef] [PubMed]
22. Tschöp, M.H. Metabolic Disease Therapies. *Cell Metab.* **2017**, *26*, 579–583.
23. Lee, C.-W.; Wong, L.L.-Y.; Tse, E.Y.-T.; Liu, H.-F.; Leong, V.Y.-L.; Lee, J.M.-F.; Hardie, D.G.; Ng, I.O.-L.; Ching, Y.-P. AMPK Promotes p53 Acetylation via Phosphorylation and Inactivation of SIRT1 in Liver Cancer Cells. *Cancer Res.* **2012**, *72*, 4394. [CrossRef] [PubMed]
24. Koundouros, N.; Poulogiannis, G. Phosphoinositide 3-Kinase/Akt Signaling and Redox Metabolism in Cancer. *Front. Oncol.* **2018**, *8*, 160–169. [CrossRef]
25. Zheng, W.; Feng, Q.; Liu, J.; Guo, Y.; Gao, L.; Li, R.; Xu, M.; Yan, G.; Yin, Z.; Zhang, S.; et al. Inhibition of 6-phosphogluconate Dehydrogenase Reverses Cisplatin Resistance in Ovarian and Lung Cancer. *Front. Pharmacol.* **2017**, *8*, 421–432. [CrossRef]

26. Rehder, D. Implications of vanadium in technical applications and pharmaceutical issues. *Inorg. Chim. Acta* **2017**, *455*, 378–389. [CrossRef]
27. Crans, D.C.; Henry, L.; Cardiff, G.; Posner, B.I. Developing Vanadium as an Antidiabetic or Anticancer Drug: A Clinical and Historical Perspective. In *Essential Metals in Medicine: Therapeutic Use and Toxicity of Metal Ions in the Clinic*, 1st ed.; Carver, P.L., Ed.; De Gruyter: Berlin, Germany; Boston, MA, USA, 2019; pp. 203–230.
28. Jakusch, T.; Kiss, T. In vitro study of the antidiabetic behavior of vanadium compounds. *Coord. Chem. Rev.* **2017**, *351*, 118–126. [CrossRef]
29. Thompson, K.H.; Orvig, C. Vanadium in diabetes: 100 years from Phase 0 to Phase I. *J. Inorg. Biochem.* **2006**, *100*, 1925–1935. [CrossRef]
30. Thompson, K.H.; Lichter, J.; LeBel, C.; Scaife, M.C.; McNeill, J.H.; Orvig, C. Vanadium treatment of type 2 diabetes: A view to the future. *J. Inorg. Biochem.* **2009**, *103*, 554–558. [CrossRef]
31. Rehder, D. Transport, Accumulation, and Physiological Effects of Vanadium. In *Detoxification of Heavy Metals*; Sherameti, I., Varma, A., Eds.; Springer: Berlin/Heidelberg, Germany, 2011; pp. 205–220.
32. Gruzewska, K.; Michno, A.; Pawelczyk, T.; Bielarczyk, H. Essentiality and toxicity of vanadium supplements in health and pathology. *J. Physiol. Pharmacol.* **2014**, *65*, 603–611.
33. Sánchez Lombardo, I.; Sánchez Lara, E.; Pérez Benítez, A.; Mendoza, Á.; Bernès, S.; González Vergara, E. Synthesis of Metforminium(2+) Decavanadates-Crystal Structures and Solid-State Characterization. *Eur. J. Inorg. Chem.* **2014**, *2014*, 4581–4588. [CrossRef]
34. Treviño, S.; González-Vergara, E. Metformin-decavanadate treatment ameliorates hyperglycemia and redox balance of the liver and muscle in a rat model of alloxan-induced diabetes. *New J. Chem.* **2019**, *43*, 17850–17862. [CrossRef]
35. Treviño, S.; Sánchez-Lara, E.; Sarmiento-Ortega, V.E.; Sánchez-Lombardo, I.; Flores-Hernández, J.Á.; Pérez-Benítez, A.; Brambila-Colombres, E.; González-Vergara, E. Hypoglycemic, lipid-lowering and metabolic regulation activities of metforminium decavanadate $(H_2Metf)_3$ $[V_{10}O_{28}]\cdot 8H_2O$ using hypercaloric-induced carbohydrate and lipid deregulation in Wistar rats as biological model. *J. Inorg. Biochem.* **2015**, *147*, 85–92. [CrossRef] [PubMed]
36. Durif, A.; Averbuch-Pouchot, M.T.; Guitel, J.C. Structure d'un Decavanadate d'Hexasodium Hydrate. *Acta Crystallogr. Sect. B Struct. Sci.* **1980**, *36*, 680–682. [CrossRef]
37. Howarth, O.W.; Jarrold, M. Protonation of the decavanadate(6-) ion: A vanadium-51 nuclear magnetic resonance study. *J. Chem. Soc. Dalton Trans.* **1978**, *5*, 503–506. [CrossRef]
38. Goddard, J.B.; Gonas, A.M. Kinetics of the dissociation of decavanadate ion in basic solutions. *Inorg. Chem.* **1973**, *12*, 574–579. [CrossRef]
39. Schwarzenbach, G.; Geier, G. 97. Die Raschacidifierung und -alkalisierung von Vanadaten. *Helv. Chim. Acta* **1963**, *46*, 906–926. [CrossRef]
40. Pascale, F.; Bedouet, L.; Baylatry, M.; Namur, J.; Laurent, A. Comparative Chemosensitivity of VX2 and HCC Cell Lines to Drugs Used in TACE. *Anticancer Res.* **2015**, *35*, 6497–6503.
41. Mohamadi, M.; Yousef Ebrahimipour, S.; Torkzadeh-Mahani, M.; Foro, S.; Akbari, A. A mononuclear diketone-based oxido-vanadium(IV) complex: Structure, DNA and BSA binding, molecular docking and anticancer activities against MCF-7, HPG-2, and HT-29 cell lines. *RSC Adv.* **2015**, *5*, 101063–101075. [CrossRef]
42. Dhahagani, K.; Mathan Kumar, S.; Chakkaravarthi, G.; Anitha, K.; Rajesh, J.; Ramu, A.; Rajagopal, G. Synthesis and spectral characterization of Schiff base complexes of Cu(II), Co(II), Zn(II) and VO(IV) containing 4-(4-aminophenyl)morpholine derivatives: Antimicrobial evaluation and anticancer studies. *Spectrochim. Acta A Mol. Biomol. Spectrosc.* **2014**, *117*, 87–94. [CrossRef]
43. Correia, I.; Adão, P.; Roy, S.; Wahba, M.; Matos, C.; Maurya, M.R.; Marques, F.; Pavan, F.R.; Leite, C.Q.F.; Avecilla, F.; et al. Hydroxyquinoline derived vanadium(IV and V) and copper(II) complexes as potential anti-tuberculosis and anti-tumor agents. *J. Inorg. Biochem.* **2014**, *141*, 83–93. [CrossRef] [PubMed]
44. Amuthan, V.D.A.; Chandrashekara, S.S.; Venkata, R.; Richard, L. Cytoprotective Activity of Neichitti (Vernonia cinerea) in Human Embryonic Kidney (HEK293) Normal Cells and Human Cervix Epitheloid Carcinoma (HeLa) Cells against Cisplatin Induced Toxicity: A Comparative Study. *J. Clin. Diagn. Res.* **2019**, *13*, KC01–KC06. [CrossRef]
45. Fujita, H.; Hirose, K.; Sato, M.; Fujioka, I.; Fujita, T.; Aoki, M.; Takai, Y. Metformin attenuates hypoxia-induced resistance to cisplatin in the HepG2 cell line. *Oncol. Lett.* **2019**, *17*, 2431–2440. [CrossRef] [PubMed]

46. Cheng, M.; Li, N.; Wang, N.; Hu, K.; Xiao, Z.; Wu, P.; Wei, Y. Synthesis, structure and antitumor studies of a novel decavanadate complex with a wavelike two-dimensional network. *Polyhedron* **2018**, *155*, 313–319. [CrossRef]
47. Li, Y.-T.; Zhu, C.-Y.; Wu, Z.-Y.; Jiang, M.; Yan, C.-W. Synthesis, crystal structures and anticancer activities of two decavanadate compounds. *Transit. Met. Chem.* **2010**, *35*, 597–603. [CrossRef]
48. Missina, J.M.; Gavinho, B.; Postal, K.; Santana, F.S.; Valdameri, G.; de Souza, E.M.; Hughes, D.L.; Ramirez, M.I.; Soares, J.F.; Nunes, G.G. Effects of Decavanadate Salts with Organic and Inorganic Cations on Escherichia coli, Giardia intestinalis, and Vero Cells. *Inorg. Chem.* **2018**, *57*, 11930–11941. [CrossRef]
49. Wang, Q.; Liu, T.-T.; Fu, Y.; Wang, K.; Yang, X.-G. Vanadium compounds discriminate hepatoma and normal hepatic cells by differential regulation of reactive oxygen species. *J. Biol. Inorg. Chem.* **2010**, *15*, 1087–1097. [CrossRef]
50. Hao, J.; Huang, K.; Chen, C.; Liang, Y.; Wang, Y.; Zhang, X.; Huang, H. Polydatin Improves Glucose and Lipid Metabolisms in Insulin-Resistant HepG2 Cells through the AMPK Pathway. *Biol. Pharm. Bull.* **2018**, *41*, 891–898. [CrossRef]
51. Ferretti, A.C.; Hidalgo, F.; Tonucci, F.M.; Almada, E.; Pariani, A.; Larocca, M.C.; Favre, C. Metformin and glucose starvation decrease the migratory ability of hepatocellular carcinoma cells: Targeting AMPK activation to control migration. *Sci. Rep.* **2019**, *9*, 2815. [CrossRef]
52. Hardie, D.G. Molecular Pathways: Is AMPK a Friend or a Foe in Cancer? *Clin. Cancer Res.* **2015**, *21*, 3836–3840. [CrossRef]
53. Lu, B.; Ennis, D.; Lai, R.; Bogdanovic, E.; Nikolov, R.; Salamon, L.; Fantus, C.; Le-Tien, H.; Fantus, I.G. Enhanced sensitivity of insulin-resistant adipocytes to vanadate is associated with oxidative stress and decreased reduction of vanadate (+5) to vanadyl (+4). *J. Biol. Chem.* **2001**, *276*, 35589–35598. [CrossRef]
54. Tardif, A.; Julien, N.; Chiasson, J.-L.; Coderre, L. Stimulation of glucose uptake by chronic vanadate pretreatment in cardiomyocytes requires PI 3-kinase and p38 MAPK activation. *Am. J. Physiol. Endocrinol. Metab.* **2003**, *284*, E1055–E1064. [CrossRef] [PubMed]
55. Žižić, M.; Miladinović, Z.; Stanić, M.; Hadžibrahimović, M.; Živić, M.; Zakrzewska, J. 51V NMR investigation of cell-associated vanadate species in Phycomyces blakesleeanus mycelium. *Res. Microbiol.* **2016**, *167*, 521–528. [CrossRef] [PubMed]
56. Zhao, Q.; Chen, D.; Liu, P.; Wei, T.; Zhang, F.; Ding, W. Oxidovanadium(IV) sulfate-induced glucose uptake in HepG2 cells through IR/Akt pathway and hydroxyl radicals. *J. Inorg. Biochem.* **2015**, *149*, 39–44. [CrossRef]
57. Seale, A.P.; de Jesus, L.A.; Park, M.C.; Kim, Y.S. Vanadium and insulin increase adiponectin production in 3T3-L1 adipocytes. *Pharmacol. Res.* **2006**, *54*, 30–38. [CrossRef] [PubMed]
58. Yraola, F.; García-Vicente, S.; Marti, L.; Albericio, F.; Zorzano, A.; Royo, M. Understanding the mechanism of action of the novel SSAO substrate $(C_7NH_{10})_6(V_{10}O_{28})\cdot 2H_2O$, a prodrug of peroxovanadate insulin mimetics. *Chem. Biol. Drug. Des.* **2007**, *69*, 423–428. [CrossRef]
59. Marín-Peñalver, J.J.; Martín-Timón, I.; Sevillano-Collantes, C.; Del Cañizo-Gómez, F.J. Update on the treatment of type 2 diabetes mellitus. *World J. Diabetes* **2016**, *7*, 354–395. [CrossRef]
60. Skelin, M.; Rupnik, M.; Cencic, A. Pancreatic beta cell lines and their applications in diabetes mellitus research. *Altex* **2010**, *27*, 105–113. [CrossRef]
61. Zhang, A.Q.; Gao, Z.Y.; Gilon, P.; Nenquin, M.; Drews, G.; Henquin, J.C. Vanadate stimulation of insulin release in normal mouse islets. *J. Biol. Chem.* **1991**, *266*, 21649–21656.
62. Proks, P.; Ashfield, R.; Ashcroft, F.M. Interaction of vanadate with the cloned beta cell K(ATP) channel. *J. Biol. Chem.* **1999**, *274*, 25393–25397. [CrossRef]
63. Gogg, S.; Chen, J.; Efendic, S.; Smith, U.; Ostenson, C. Effects of phosphotyrosine phosphatase inhibition on insulin secretion and intracellular signaling events in rat pancreatic islets. *Biochem. Biophys. Res. Commun.* **2001**, *280*, 1161–1168. [CrossRef] [PubMed]
64. Chen, J.; Ostenson, C.G. Inhibition of protein-tyrosine phosphatases stimulates insulin secretion in pancreatic islets of diabetic Goto-Kakizaki rats. *Pancreas* **2005**, *30*, 314–317. [CrossRef] [PubMed]
65. Liu, H.-K.; Green, B.D.; McClenaghan, N.H.; McCluskey, J.T.; Flatt, P.R. Long-Term Beneficial Effects of Vanadate, Tungstate, and Molybdate on Insulin Secretion and Function of Cultured Beta Cells. *Pancreas* **2004**, *28*, 264–268. [CrossRef] [PubMed]

66. Zhao, Y.; Ye, L.; Liu, H.; Xia, Q.; Zhang, Y.; Yang, X.; Wang, K. Vanadium compounds induced mitochondria permeability transition pore (PTP) opening related to oxidative stress. *J. Inorg. Biochem.* **2010**, *104*, 371–378. [CrossRef]
67. Hosseini, M.J.; Shaki, F.; Ghazi-Khansari, M.; Pourahmad, J. Toxicity of vanadium on isolated rat liver mitochondria: A new mechanistic approach. *Metallomics* **2013**, *5*, 152–166. [CrossRef]
68. Soares, S.S.; Gutiérrez-Merino, C.; Aureliano, M. Mitochondria as a target for decavanadate toxicity in Sparus aurata heart. *Aquat. Toxicol.* **2007**, *83*, 1–9. [CrossRef]
69. Crans, D.C.; Bunch, R.L.; Theisen, L.A. Interaction of trace levels of vanadium(IV) and vanadium(V) in biological systems. *J. Am. Chem. Soc.* **1989**, *111*, 7597–7607. [CrossRef]
70. Griffin, E.; Levina, A.; Lay, P.A. Vanadium(V) tris-3,5-di-tert-butylcatecholato complex: Links between speciation and anti-proliferative activity in human pancreatic cancer cells. *J. Inorg. Biochem.* **2019**, *201*, 110815. [CrossRef]
71. Aureliano, M.; Tiago, T.; Gândara, R.M.C.; Sousa, A.; Moderno, A.; Kaliva, M.; Salifoglou, A.; Duarte, R.O.; Moura, J.J.G. Interactions of vanadium(V)–citrate complexes with the sarcoplasmic reticulum calcium pump. *J. Inorg. Biochem.* **2005**, *99*, 2355–2361. [CrossRef]
72. Sánchez-Lombardo, I.; Baruah, B.; Alvarez, S.; Werst, K.R.; Segaline, N.A.; Levinger, N.E.; Crans, D.C. Size and shape trump charge in interactions of oxovanadates with self-assembled interfaces: Application of continuous shape measure analysis to the decavanadate anion. *New J. Chem.* **2016**, *40*, 962–975. [CrossRef]
73. Student, A.K.; Hsu, R.Y.; Lane, M.D. Induction of fatty acid synthetase synthesis in differentiating 3T3-L1 preadipocytes. *J. Biol. Chem.* **1980**, *255*, 4745–4750. [PubMed]